Journal of Applied Sciences

ISSN 1812-5654

science alert

ANSInet
an open access publisher
http://ansinet.com

Journal of Applied Sciences 13 (7): 1052-1058, 2013
ISSN 1812-5654 / DOI: 10.3923/jas.2013.1052.1058

Aerodynamic Performance of Nozzle Blade Cascade with Meridian-shrank Endwall Profile

Feng Zi-Ming, Zhang Jin-Dong and Gu Hui-Bin
School of Mechanical Science and Engineering, Northeast Petroleum University,
Daqing, Heilongjiang, 163318, China

Abstract: In order to improve aerodynamic performance and internal efficiency of turbine, the nozzle straight blade was reformed into meridian-shrank blade that the endwall profile was redesigned to improve its fluid flow performance and internal efficiency. Simulation results shown that meridian-shrank design of the end wall outer profile could form uniform static pressure distribution along the blade height and restrained the development of radial secondary flow of the boundary layer. The pressure loss of meridian-shrank blade was less than straight blade from 0 to 0.89 relative blade height and a little more than straight blade near the blade tip. Overall, the meridian-shrank blade could improve its aerodynamic efficiency and this technology can provide theoretical guidance to design machinery with high performance.

Key words: Nozzle blade cascade, meridian-shrank blade, secondary flow, efficiency

INTRODUCTION

Turbomachinery were the critical component of important equipment such as steam turbine, gas turbine and aero-engine and had very important function in the national economy and national defense. Its internal flow research was concerned by the domestic and overseas scholars. It could be said that the research of the internal flow in turbomachinery still was one of the most active areas of research (Zhao *et al*., 2013; Liu *et al*., 2012; Flores *et al*., 2010).

In the past decades, many researchers had studied the secondary flow in different types of turbine and compressor cascade and had clearly understanding secondary flow loss mechanism. The representation of flow of Longston (Langston, 1980) was generally accepted by most people. Obviously, if all the sources of arousing flow loss could be controlled, it was very beneficial to reduce the secondary flow in cascade. A reasonable endwall profile was one of effective means to control secondary flow. The general using technology of meridian-shrank blade in turbomachinery was the best examples of this research direction (Lakshminarayana *et al*., 1986; Tran, 1986; Warner and Tran, 1987). In fact, this method was putted forward in the first time by Deich *et al*. (1960) in the early 1960s. Its purpose was to improve flow near the endwall by redesign endwall profile, thereby improve the secondary flow and improve turbine efficiency. Haas and Boyle (1984) studied a set of turbine static cascade with little load blade profile and respectively tested straight line shrank endwall and S-type shrank endwall. The static blade flow angle distribution along span shown that the flow angle near blade tip was slightly over-deflected, the tip flow efficiency was slightly lower. Kopper *et al*. (1980) tested a set of turbine cascade, the meridian-shrank endwall was adopted axisymmetric profile like Morris and Hoare and its aerodynamic performance was compared with the conventional parallel-plate cascade endwall. The results indicated that the leading edge aerodynamic load of turbine cascade was reduced, the lowest pressure point moved to the near trailing edge, the adverse pressure gradient at the line side decreased from lowest pressure point to the trailing edge and increased at the profile line side. Petrovic *et al*. (2000) optimized a turbine stage with meridian-shrank method and the stage efficiency was increased by 2%.

The purpose of this study designed a meridian-shrank endwall at the rear of the cascde laryngeal in order to decrease the flow separation of diffusion section near the cascade outlet and make the gas flow accelerating that the radial pressure gradient was decreased by changing the curvature of streamline in order to control and eliminate the secondary flow loss of cascade and improve the efficiency of turbomachinery.

BLADE MODEL AND COMPUTATION BOUNDARY CONDITION

This CFD simulation was conducted with ANSYS-CFX software and the mesh was generated by

Corresponding Author: Feng Ziming, School of Mechanical Science and Engineering, Northeast Petroleum University, Daqing, Heilongjiang, 163318, China

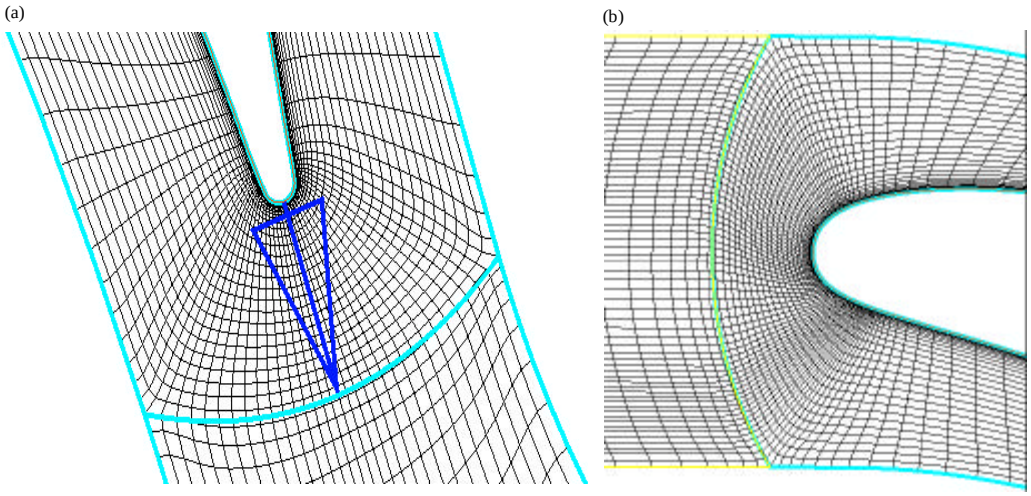

Fig. 1(a-b): Part computational grid, (a) Part grid of trailing edge and (b) Part grid of leading edge

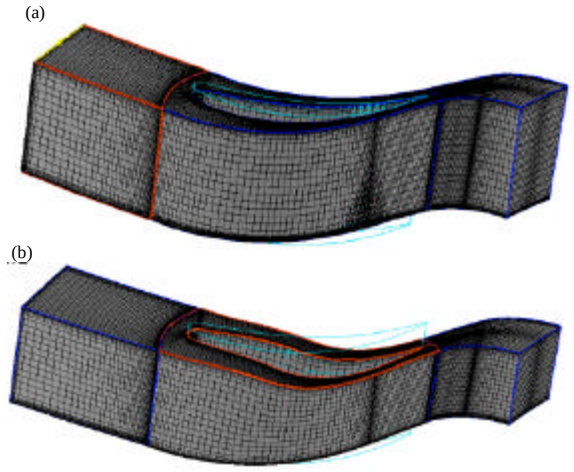

Fig. 2(a-b): Three-dimensional grid of computational domain, (a) Straight blade and (b) Meridian shrank blade

AUTOGRID software. Figure 1 was part mesh of the leading edge and trailing edge. Figure 2 stood for 3D structural grid model that was make of three grid blocks of H, O and I type grid, so it was named H-O-I type grid. O-grid could be converted into H-grid with a certain topological transformation, it was fitted for the turbomachinery cascade structure with fine capacity of simulating wake flow. The grid orthogonality, aspect ratio and total number of grid nodes were, respectively 35.25°, 134 and 410000 that meet the CFX mesh quality requirements. Boundary conditions were as followed; inlet total pressure was 103065 Pa, inlet total temperature was 316 k, outlet static pressure was 0.1 MPa, turbulence model was Spalart-Allmaras model.

Table 1: Blade geometry and aerodynamic parameters

Name	Value
Outer diameter (mm)	$D_t = 3275$
Middle diameter (mm)	Dm = 3197.5
Inner diameter (mm)	$D_h = 3120$
Blade height (mm)	h = 155
Diameter height ratio	$D_m/h = 20.6$
Chord length (mm)	b = 299.5
Pitch length (mm)	t = 104.28
Axial chord length (mm)	B = 299.5
Aspect ratio	t/b = 0.35
Span chord ratio	h/b = 0.52
Blade number	N = 64
Blade inlet angle	$\alpha_0 = 90$
Blade outlet angle	$\alpha_1 = 15°$
Coming total pressure (gauge pressure) (Pa)	$P_0^* = 3195$
Mach number at middle blade	Ma = 0.20
Reynolds number	$Re = 4.9\times10^5$

The main geometry and aerodynamic parameters of cascade were shown in Table 1.

CASCADE CFD SIMULATION VERIFICATION

Figure 3 and 4 compared the simulation curves of static pressure coefficient (Cps) and total pressure loss coefficient (Cpt) with test curves, respectively. The results indicated that the error was in the reasonable region. The error was mainly induced by the deviation between computed incidence and test incidence and computed method. But the distribution pattern of the two curves were nearly similar with each other, it was proved that CFX could be used to simulate the internal flow field of turbomachinery.

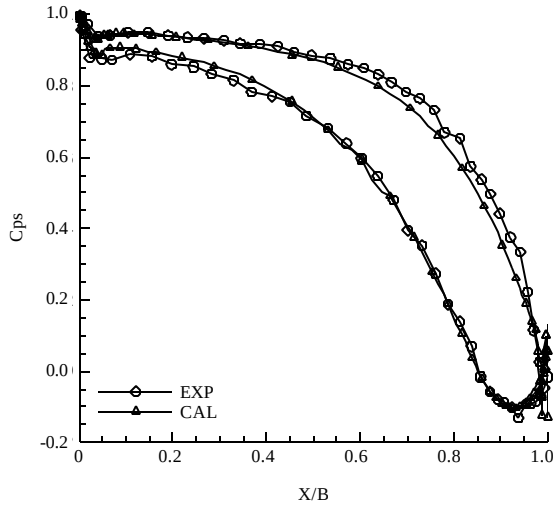

Fig. 3: Cps distribution in the blade profile

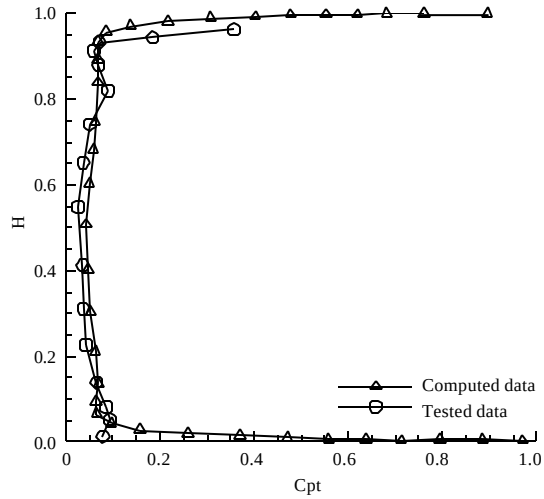

Fig. 4: Picth-averaged Cpt distribution along span

Figure 5 stood for the test and simulated results of tip endwall surface streamline. As the Fig. 5a and b shown that the numerical simulation of leading saddle point position, the tow separation lines of horseshoe vortex branch of suction surface and of pressure surface position, entering into suction surface and streamline direction, were coincided very well with experimental results.

Therefore, the NUMECA software can be used to simulate the internal flow field of turbomachinery and qualitatively and quantificationally reflected reality flow status.

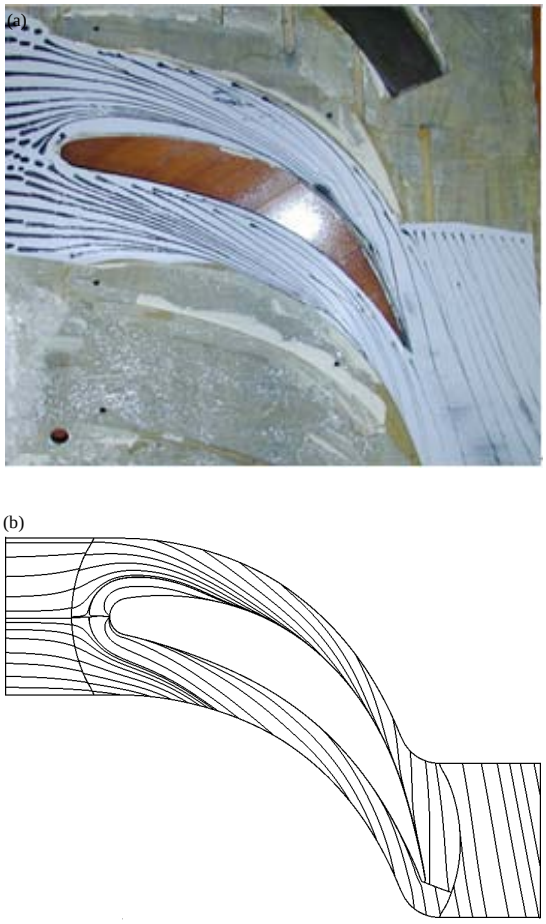

Fig. 5(a-b): Tip endwall streamline, (a) Test result and (b) Computation result

ANALYSIS OF COMPUTING RESULT

Cps distribution along blade profile: As Fig. 6-8 shown, the area surrounded by Cps of MSB was smaller than PB, it meant that blade load of MSB was smaller than PB. Usually flow loss around cascade was proportional to blade load, the flow loss of MSB cascade was smaller than PB. Crosswise pressure gradient of MSB cascade was smaller than PB and reached the maximum near 95% relative axial chord length, but the maximum of PB was achieved at the 90% relative axial chord length. The two crosswise pressure gradient of MSB and PB were all little, therefore it didn't happen that the endwall boundary layer was accumulated in the endwall corner of cascade suction surface.

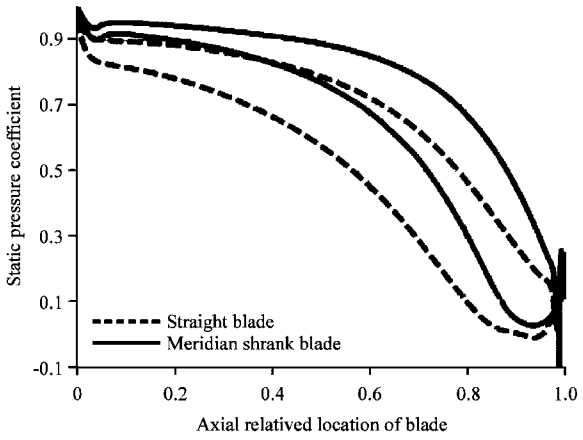

Fig. 6: Cross profile at 10% blade height

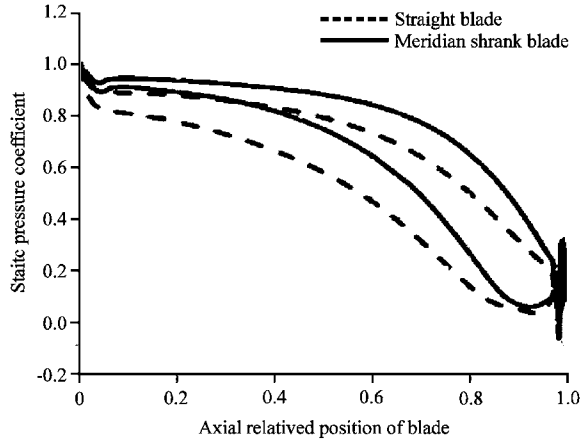

Fig. 7: Cross profile at 50% blade height

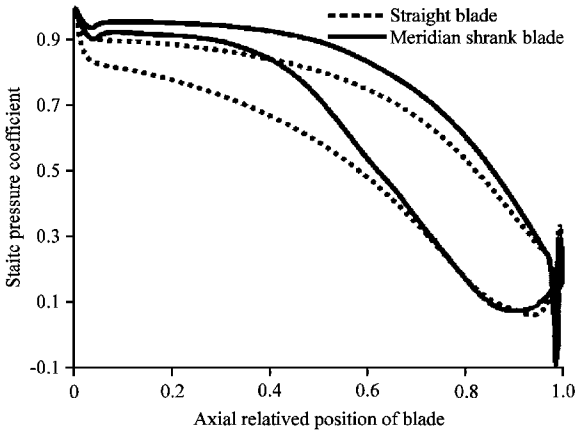

Fig. 8: Cross profile at 90% blade height

As Fig. 9 shown, the suction side lowest pressure point at arbitrary blade height of MSB were all located in the scope of 90~95% relative axial chord. According to

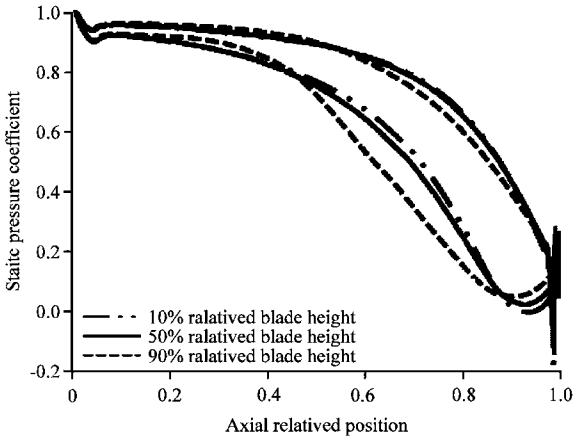

Fig. 9: Cps of MSB distribution along profile

aft-load profile definition, if the lowest pressure point of profile was located after relative axial chord, it was aft-load profile. Obviously, the designed nozzle cascade blade in this study all had aft-load profile. As to cascade with aft-load profile, most (90~95%) boundary layer in the suction side and pressure side was accelerating by accelerating pressure gradient with slow incrassation. When suction side boundary layer with a certain thickness encounter adverse pressure gradient at the trailing edge, the flow would be transited into turbulent flow in the downstream flow field. Therefore there was a little turbulent flow area in boundary layer in the blade surface with aft-load profile.

Cps isoline distribution in the blade surface: As to PB cascade shown in Fig. 10, most Cps isoline was straight line and perpendicular to tip and down endwalls. It indicated that static pressure distribution was roughly uniform along blade height. Static pressure field essentially presented bidimensional flow. It was laminar region near endwalls. Cps isoline was closed after entering into adverse pressure gradient, it indicated that this flow region was three-dimensional flow and high flow loss area.

The MSB obviously changed the Cps isoline distribution. Cps isoline was bended in the meridian surface. The crosswise pressure gradient would be very weak because of the blade cascade adopted aft-load profile and the passage vortex would happen at lower blade height near the trailing edge. Therefore, there was not secondary flow along blade height and the secondary flow in cascade was just crosswise secondary flow loss of endwalls.

Outlet pitch-average Cpt distribution along span: Comparing the two curves in Fig. 11, it was clearly seen

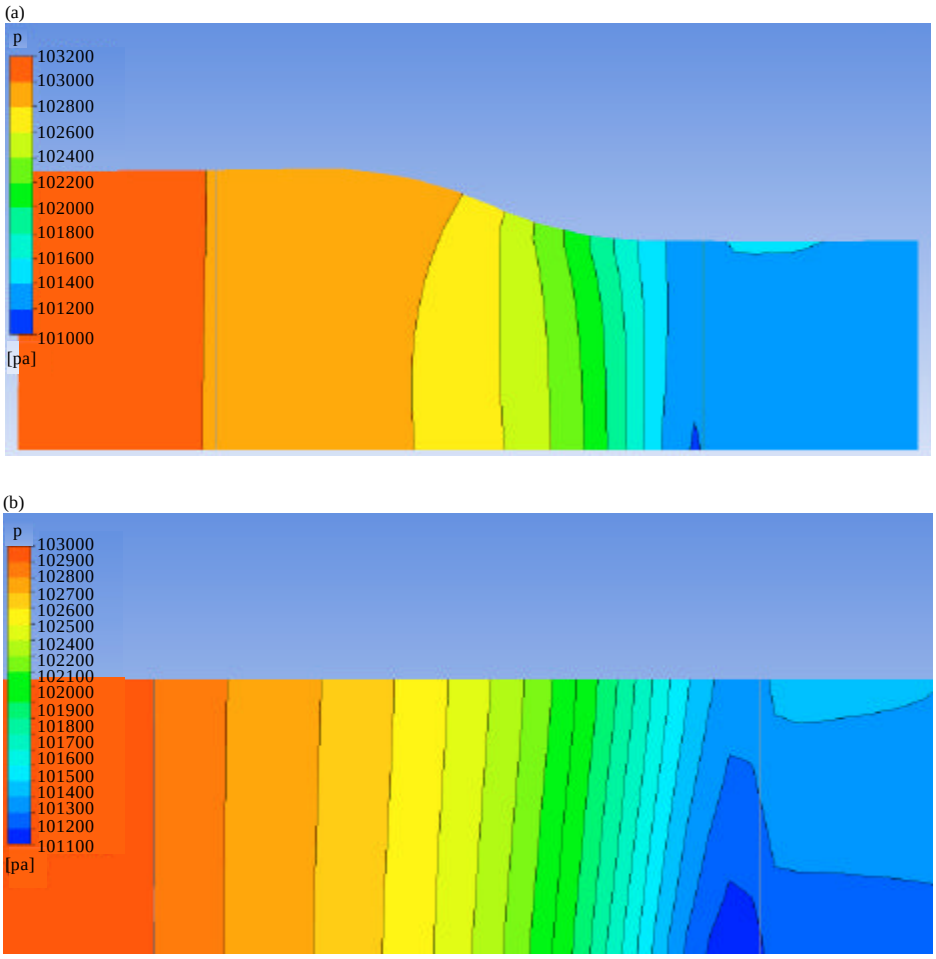

Fig. 10(a-b): Pitch-average Cps distribution, (a) Meridian shrank blade and (b) Straight blade

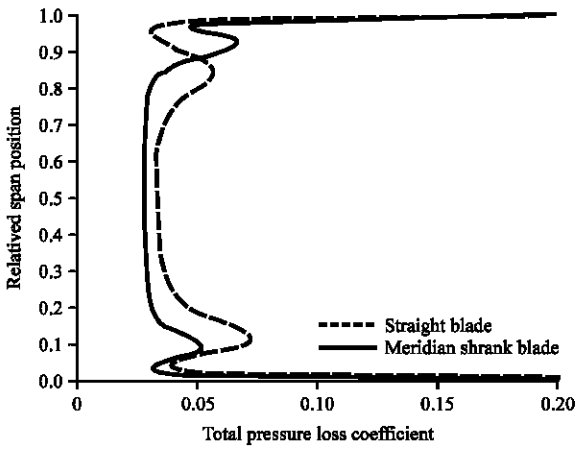

Fig. 11: Cpt Distribution along Span

that there were three regions, root, tip and middle blade, from root to tip of blade. In the root and middle blade regions, total pressure loss of PB was greater than MSB. In the tip blade region, the total pressure loss of MSB was greater than PB. The flow loss peak at about 10% relative blade height was aroused by down endwall passage vortex and was justly corresponding to the passage vortex core. The loss peak of PB was greater than MSB, it indicated that passage vortex of PB was intensity much more than MSB. The passage vortex near blade tip also formed a loss peak. The passage vortex near tip endwall of MSB formed a high loss region more near the tip endwall than PB and nearly connected one region with endwall boundary layer loss. It was because that the crosswise pressure gradient increased and endwall boundary layer was incrassated after entering into rear section of axial position, passage vortex was uplifted a

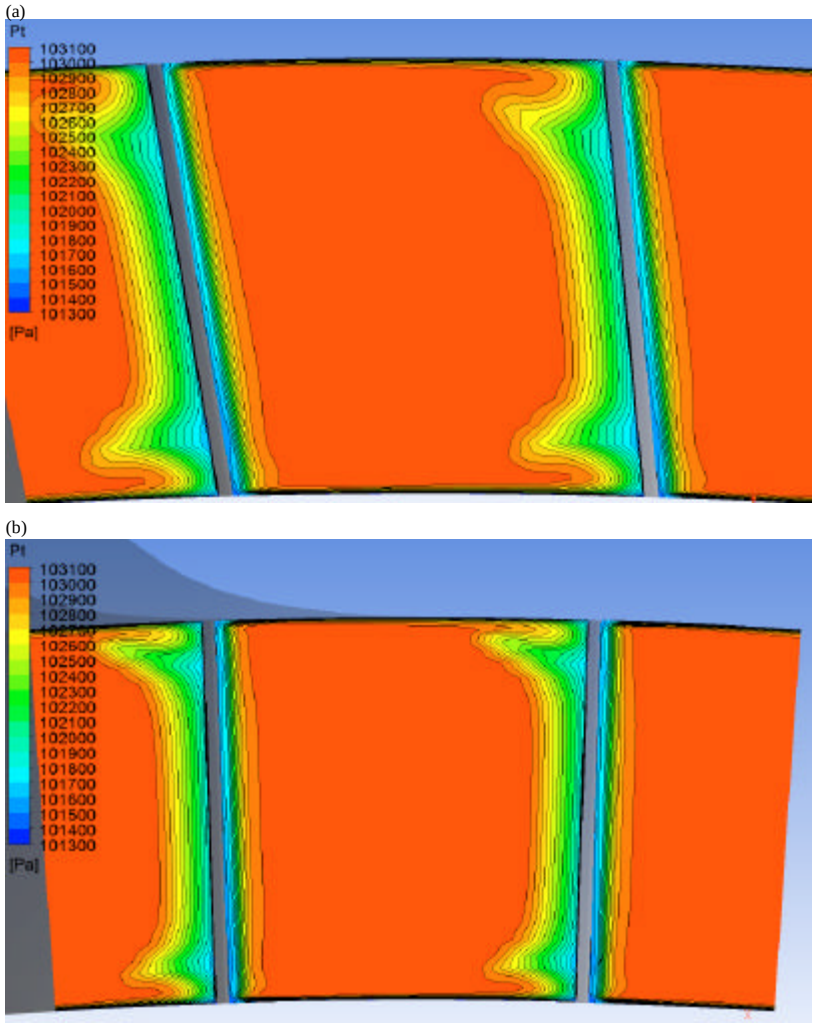

Fig. 12: Cpt isoline distribution in the outlet cross section, (a) Meridian-shrank blade and (b) Prototype blade

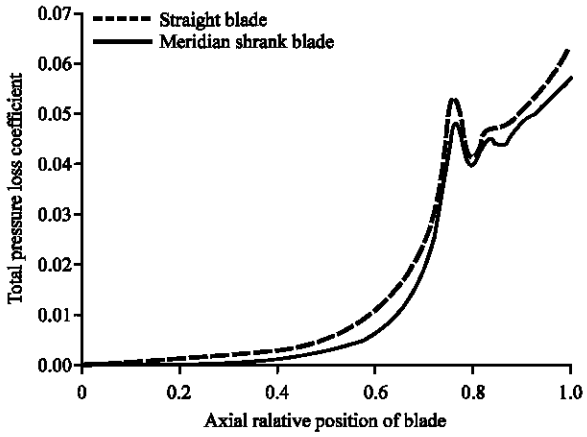

Fig. 13: Cpt distribution along axial direction

little, so it made higher pressure loss. MSB made the flow accelerating in cascade passage so that the pressure difference was decreased in the most region of blade surface along span and the boundary layer thickness increased slowly. Therefore middle blade flow loss of MSB was less than PB cascade.

Cpt isoline distribution in outlet cross section: As Fig. 12 shown, the high flow loss area of PB and MSB were all located in tip and down endwall and waking flow. Comparing to two flow loss cores of PB, two flow loss cores of MSB were relatively little and were more nearer to tip and down endwall. It was obvious that high flow loss area of PB was bigger than MSB and its width of the whole high loss area along span was littler too than PB.

Cpt distribution along axial direction: The Cpt distribution along axial direction of PB and MSB were shown in Fig. 13. The Cpt increased unclearly in the beginning stage in the inlet of cascade passage and increased severely from 0.63 relative axial chord length to blade trailing edge because of main passage vortex formation and boundary layer incrassation by outlet diffusion section. Cpt could continue to increase near outlet because gas flow from suction side was severely mixed with gas flow from pressure side near outlet. Cpt of MSB was lower than PB at the same location. PB cascade total flow loss was about 6.35% and its flow efficiency was 93.65%. MSB cascade total flow loss was about 5.8% and its flow efficiency was 94.2%. Comparing to PB cascade, The MSB cascade flow efficiency was increased 0.55%.

CONCLUSION

Simulation results indicated that aerodynamic performance parameters of nozzle blade cascade were all working in reasonable condition and every flow loss were not big. The spilled-type meridian-shrank design with outer endwall formed Cps distribution along span that restrained radial secondary flow of boundary layer. The blade had aft-load profile, its lowest pressure point located after 90% axial chord length that markedly decreased crosswise pressure gradient in the passage and decreased crosswise secondary flow loss near endwall. This aft-load profile reflected the excellent aerodynamic performance of meridian-shrank blade. Seeing from Cpt distribution along span, pressure loss in the scope of 0%~89% blade height of meridian-shrank blade was less than the PB cascade and increased only in the blade tip. Seeing from total pressure loss comparison, meridian-shrank blade decreased flow loss and its efficiency was increased by 0.55%.

NOMENCLATURE

Cps = Static Pressure Coefficient = Static pressure/Incoming Total Pressure before Cascade
PB = Prototype Blade
MSB = Meridian-Shrank Blade
Cpt = Total Pressure Loss Coefficient

REFERENCES

Deich, M.E., A.E. Zaryankin, G.A. Eilippov, 1960. Method of increasing the efficiency of turbine stages with short blade. A.E.I. Trans., l2: 18-24.

Flores, J.G., G. Urquiza and J.A. Hernandez, 2010. Inverse neural network to optimal performance of the hydraulic turbine runner blades. Int. J. Adv. Comput. Technol., 2: 47-56.

Haas, J.E. and R.J. Boyle, 1984. Analytical and experimental investigation of stator endwall contouring in a small axial flow turbine. NASA Technical Paper No. TP-2309, pp: 1-20.

Kopper, F.C., R. Milano and M. Vanco, 1980. An experimental investigation of endwall profiling in a turbine vane cascade. Proceedings of the 16th AIAA, SAE and ASME, Joint Propulsion Conference, June 30-July-2, 1980, Hartford, Connecticut, pp: 1-10.

Lakshminarayana, B., N. Sitaram and J. Zhang, 1986. End-wall and profile losses in a low-speed axial flow compressor rotor. J. Eng. Gas Turbines Power, 108: 22-31.

Langston, L.S., 1980. Cross flows in a turbine cascade passage. ASME J. Eng. Power, 102: 866-877.

Liu, Q., H. Zheng, L. Cai, Q. Long and R. Yang, 2012. CFD modeling of exhaust heat recovery using methane steam reforming in steam reformer of chemically recuperated gas turbine. JCIT, 7: 152-161.

Petrovic, M.V., G.S. Dulikravich and T.J. Martin, 2000. Maximizing multistage turbine efficiency by optimizing hub and shroud shapes and inlet and exit conditions of each blade row. Int. J. Turbo Jet Engines, 17: 267-278.

Tran, M.H., 1986. Recent development in blading to improve turbine efficiency. American Society of Mechanical Engineers, USA., pp: 1-8.

Warner, R.E. and M.H. Tran, 1987. Recent development to improve high pressure and intermediate-pressure turbine efficiency. IMech EC287/87, pp: 1-10.

Zhao, X., L. Zhao and B. Louis, 2013. Analysis on service life of hot-end components of gas turbine using equivalent operation. Int. J. Adv. Comput. Technol., 5: 975-980.